ISSN 1028-334X, Doklady Earth Sciences, 2007, Vol. 413A, No. 3, pp. 462–468. © Pleiades Publishing, Ltd., 2007.
Original Russian Text © I.S. Peretyazhko, E.A. Tsareva, V.Ye. Zagorsky, 2007, published in Doklady Akademii Nauk, 2007, Vol. 413, No. 6, pp. 791–797.

GEOCHEMISTRY

A First Finding of Anomalously Cs-Rich Aluminosilicate Melts in Ongonite: Evidence from Melt Inclusion Study

I. S. Peretyazhko, E. A. Tsareva, and V. Ye. Zagorsky

Presented by Academician M.I. Kuz'min May 18, 2006

Received May 29, 2006

DOI: 10.1134/S1028334X07030324

The chemical properties of cesium allow accumulation of this element in the late silicic derivatives of igneous complexes, in particular, in rare-metal granites, pegmatites, and related metasomatic rocks. However, the Cs content can be high enough only in pegmatites to form its own mineral (pollucite), which occasionally occurs in considerable amounts. In other rocks, Cs concentrates largely in micas and feldspars. The possible maximal level of Cs accumulation in the melt remains poorly studied. Important new information has been obtained from the study of volcanic glass and melt inclusions (MI) in minerals. The rhyolitic glass concentrates 220–870 ppm Cs, occasionally up to 3770 ppm [1]. To date, the highest Cs_2O content (1.2–5.5 wt %) has been detected in MIs captured by quartz from miarolitic pegmatite of the Malkhan field of the central Transbaikal region [2, 3] and the southwestern Pamirs (Leskhozovskaya and Vezdarinskaya veins). These inclusions contain products of crystallization of the late pegmatitic melt [3] and the inferred high-temperature meltlike gels [4]. While studying ongonite of the Ary-Bulak Massif, we detected MIs filled with a residual glass that contains up to 17 wt % Cs. This is reliable evidence in favor of the existence of natural melts extremely enriched in Cs. In this communication, we describe these unusual inclusions and discuss Cs distribution in ongonites.

The Ary-Bulak Massif is a dome-shaped stock exposed over ~0.8 km^2 among the Devonian volcanosedimentary rocks [5]. The massif is composed largely of porphyritic ongonite. A zone of aphyric rock 50–100 m wide occurs only near the southwestern contact zone. Beyond this zone, an ongonite variety with anomalously high contents of CaO (3.3–21.8 wt %) and F (2.7–16 wt %) has been found near the same locality. The high CaO (7.8–18 wt %) and F (7.1–15.5 wt %) contents are inherent to aphyric rocks as well. Prosopite $CaAl_2F_4(OH)_4$ has been identified in this rock for the first time as an abundant mineral (6–26 wt %). It was established that interstices between minerals of the groundmass of the Ca- and F-rich rocks are filled with submicrometric intergrowths of "fluoritic" and "K-feldspathic" phases. The "fluoritic" phase is a partly devitrified calcium fluoride melt with the following admixtures (wt %): O (3–12), Al (0.5–3.3), Si (0.2–1.5), Sr (0.3–0.5, occasionally up to 1.0–1.3), Na (up to 0.5), and S (up to 0.3). The "K-feldspathic" phase is commonly close in composition to sanidine (rims around tabular albite crystals) but characterized by local enrichment in Ca (1.5–4.0 wt %). We provided evidence for the joint crystallization of immiscible aluminosilicate and calcium fluoride melts in the presence of HF-bearing aqueous fluid during formation of Ca- and F-rich rocks [6, 7].

The Cs content in rocks from the Ary-Bylak Massif varies from 48 to 386 ppm. The lowest average Cs content is characteristic of the porphyritic ongonite with the "fluoritic" phase (87 ppm, average of 4 samples). Porphyritic ongonite from the central part of the massif contains 104 ppm Cs (average of 35 samples [8]). The aphyric rocks are distinguished by a high dispersion of Cs contents ranging from 82 to 386 ppm (average 159 ppm, based on 9 samples). The main amount of Cs is concentrated in feldspars (largely, sanidine). Mica of the biotite–zinnwaldite series is the only mineral with high Cs content (0.2–0.5 wt % Cs_2O, on average; up to 2–3 wt % in the narrow outer rims of some phenocrysts). However, the percentage of mica phenocrysts does not exceed fractions of a percent. The elevated Cs content (up to 250–300 ppm) in the groundmass indicates that this element was gained in the ongonite melt at the final stage of its crystallization.

Quartz phenocrysts in porphyritic ongonite contain numerous MIs. Anomalously high Cs contents were detected in some melt inclusions filled with a residual glass. Such unusual melt inclusions have been found in every fourth thoroughly studied rock samples taken

Vinogradov Institute of Geochemistry, Siberian Division, Russian Academy of Sciences, ul. Favorskogo 1a, Irkutsk, 664033 Russia; e-mail: pgmigor@igc.irk.ru

Table 1. Chemical composition of porphyritic rocks from the Ary-Bulak Massif, wt %

Component	1			2
	ARB-28	ARB-22	ARB-23	ARB-24
SiO_2	72.79	71.25	71.48	62.60
TiO_2	0.02	0.11	<0.02	<0.02
Al_2O_3	15.69	15.66	15.53	14.20
Fe_2O_3	0.61	0.51	0.65	<0.10
FeO	0.09	0.52	0.27	0.68
MnO	0.05	0.04	0.05	0.04
MgO	0.03	0.44	0.31	0.09
CaO	0.19	0.29	0.75	9.26
Na_2O	3.79	3.76	3.85	3.15
K_2O	4.62	4.86	4.74	4.04
Li_2O	0.11	0.10	0.11	0.08
Rb_2O	0.22	0.23	0.23	0.16
Cs_2O	0.007	0.020	0.020	0.013
P_2O_5	0.03	0.03	0.02	0.05
F	1.22	2.20	2.00	6.80
$H_2O^{\pm}$	1.05	0.94	0.86	1.46
CO_2				0.22
Total	100.01	100.03	100.03	99.98
A/NK	1.39	1.31	1.35	1.49

Note: (1) Porphyritic ongonite, (2) porphyritic ongonite with "fluoritic" phase. The total is given with correction for the F content. (–) Not analyzed. A/NK = $Al_2O_3/(Na_2O + K_2O + Cs_2O + Rb_2O)$, molar ratio. Analyses were performed at the Institute of Geochemistry, Irkutsk (G.A. Pogudina, analyst).

from the central part of the massif (ARB-28) and in its southwestern contact zone (ARB-22, ARB-23, and ARB-24). Samples ARB-28, ARB-22, and ARB-23 are composed of ordinary porphyritic ongonite, while sample ARB-24 is composed of Ca- and F-rich porphyritic rocks containing ~13 wt % of "fluoritic" phase (Table 1). Large (1–5 mm) phenocrysts of sanidine, albite with sanidine rims, well-developed smoky quartz, and sporadic colorless topaz occupy up to 20 vol %. The mica sheets are extremely rare. The phenocrysts are incorporated into the groundmass that consists of small (20–80 μm) grains of minerals scattered as phenocrysts. Aggregates of fine-acicular topaz crystals are observed in microporous domains of the rock. Numerous inclusions of acicular topaz (<1 × 3–15 μm) are contained in quartz microlites. In the Ca- and F-rich rock (sample ARB-24), interstices are filled with submicrometric intergrowths of fluoritic and "K-feldspathic" phases probably formed as quenching of products of calcium fluoride and aluminosilicate melt microemulsions [6, 7].

A few hundred quartz grains and a few topaz grains have been examined in each sample. Some of the large quartz phenocrysts are broken by rounded fractures that do not extend beyond quartz. We suppose that the fracturing was a result of $\beta \rightarrow \alpha$ quartz transition in the process of phenocryst growth. Many quartz and topaz grains contain MIs varying from 2–5 to 100–150 μm (occasionally up to 300 μm) in size. Most melt inclusions make up clusters and chains in growth zones at margins of quartz phenocrysts. Melt inclusions in central and transitional zones are rare. In many grains, melt inclusions occur together with gas-rich fluid inclusions (FI) consisting of a large bubble and a thin outer rim of solution. The rare secondary FIs were observed along the sealed fractures in only a few grains. Most MIs are filled with brownish, occasionally translucent residual glass and a deformed shrink bubble. Many MIs contain one or several crystalline phases (brown mica, potassium feldspar, and albite).

Upon heating to 360–380°C, the smoky quartz grains become colorless in 10–15 min. The residual glass in MI begins to melt at 450–500°C. Further stepwise heating was performed in a micromuffle with quenching at every stage. The complete melting of the residual glass was achieved at 700–750°C during 1–2 h. Many small (3–5 μm) inclusions became completely homogeneous thereby. At this stage, one can see that proportions of the volumes occupied by the gas bubble, crystalline phases, and melt are appreciably different even in the closely spaced MI within one group or in the same growth zone. The heating to 760–810°C over 12–30 h resulted in dissolution of mica and partial melting of feldspars. In many MIs, a titanomagnetite rash appears on the spot of mica. The complete melting of crystalline phases was reached in 30–35 h at 850–950°C. Some MIs 10–40 μm in size contained only a homogeneous melt after heating to 900–950°C. Most inclusions, especially large ones (>40 μm), did not achieve complete homogenization even at 1000–1050°C during 1–2 h, and a large gas bubble remained in glass after its quenching.

The composition of melt inclusions was determined on a LEO-1430VP SEM equipped with an INCAEnergy 300 analyzer. The residual and quenched glasses in most MIs have aluminosilicate composition with wide variations in Si, Al, Na, K, and F contents. MIs with anomalously Cs-rich glasses (0.5–17.5 wt %) were found in every sample (Table 2). In total, 11 such inclusions were detected in 9 quartz phenocrysts. These inclusions are isolated or occur together with ordinary MIs and FIs in both the inner and outer zones of quartz grains. In contrast to the ordinary MIs, the Cs-rich inclusions are usually filled with translucent or transparent residual glass. They contain one or several (up to six) large shrink cavities. Some melt inclusions contain crystalline phases.

A considerable volume in MI 22/2-2 is occupied by segregation of brown mica. After the heating to 1050°C, grains (1–5 μm) of newly formed titanomagnetite arose on the spot of mica. The dissolution of mica stimulated the saturation of the melt with Fe (up to

Table 2. Chemical composition of cesium aluminosilicate glasses from melt inclusions in quartz phenocrysts, wt %

Component	1	2					3				4		
	22/2-2	23/1-1	23/1-1a	23/1-5	23/2-3	23/4	24/1	24/1a	24/8	24/10-4	28/3-1	28/6-1	28/6-1a
SiO_2	68.16	69.15	63.02	75.43	68.70	70.39	58.55	54.20	59.03	58.73	60.56	53.35	58.23
Al_2O_3	12.93	12.79	16.15	10.93	14.92	14.76	18.80	17.86	18.24	19.87	21.70	16.83	21.02
FeO	5.80	0.19	0.41		0.69			0.89			0.86		
MnO	0.59							1.95			0.60		
Na_2O	3.73	3.73	4.49	3.24	4.58	5.21	5.68	5.78	5.49	4.32	4.62	4.43	4.85
K_2O	4.70	3.04	3.38	3.03	5.44	4.74	4.76	4.08	3.93	5.79	4.19	0.52	4.79
Cs_2O	0.53	7.33	7.18	3.03	0.63	1.41	4.10	7.17	6.55	0.96	1.48	17.51	4.29
Rb_2O		0.55	0.50				1.91		3.47				
Li_2O		0.13	0.17				0.19						
B_2O_3		0.31	0.46				0.25						
Cl			0.16	0.24	0.23		0.60	5.71	0.32	1.26			
F	4.02	3.75	5.15	4.20	2.87	4.77	5.78	6.02	6.70	7.63	4.92	14.13	7.67
H_2O		0.64	0.62				0.61						
CuO		0.59	1.07		0.65								
Total	98.77	100.61	100.55	98.29	97.44	99.26	98.67	99.84	100.84	95.07	96.85	100.80	97.63
N	2	7	14	1	6	3	4	2	3	1	3	3	6
A/NK	1.13	1.03	1.16	1.13	1.09	1.04	1.10	1.08	1.04	1.45	1.71	1.19	1.43
T, °C	1050	950		950	950	–	–		–	730	850	730	

Note: (1) Melt inclusions from sample ARB-22; (2) four melt inclusions in three quartz phenocrysts from sample ARB-23; analyses 23/1-1 and 23/1-1a characterize different areas of the same inclusion; (3) three melt inclusions in different quartz phenocrysts from sample ARB-24; analysis 24/1a characterizes an area in glass with a phase (5 μm) enriched in Cs and Cl; (4) three melt inclusions in two quartz phenocrysts from sample ARB-28. The total is given with correction for the F and Cl contents. (*N*) Number of analyses; (*T*, °C) the maximum temperature of heating; (–), without heating. A/NK = $Al_2O_3/(Na_2O + K_2O + Cs_2O + Rb_2O)$, molar ratio. Gaps in the table correspond to the contents below the detection limit (Li_2O, B_2O_3, and H_2O were not determined). CaO < 0.2 wt % in all analyses. Li_2O, Rb_2O, B_2O_3, and H_2O were determined with SIMS; Rb_2O in analysis 24/8 was determined with SEM EDS (measurement conditions for all elements: beam diameter 1–10 μm, accelerating voltage 20 kV, and current 0.3–0.5 nA, spectra setting time 50 s) at the Geological Institute, Ulan-Ude (N.S. Karmanov, analyst).

5.8 wt % FeO, see Table 2). A crystal of Na-sanidine 5 × 7 μm in size was opened in the residual (unheated) glass (MI 23/4). Its composition is as follows (wt %): 67.45 SiO_2, 18.93 Al_2O_3, 6.93 K_2O, and 6.90 Na_2O (total 100.21). The unheated glass from MI 24/8 with 6.6 wt % Cs_2O and 3.5 wt % Rb_2O contains an Rb- and Cs-rich mica crystal with the following composition (wt %): 45.86 SiO_2, 22.62 Al_2O_3, 6.98 FeO, 0.65 MnO, 8.69 K_2O, 0.54 Na_2O, 2.84 Rb_2O, 0.36 Cs_2O, and 8.21 F. The sum total (–F = O_2) is 93.25. The inner wall of the opened gas bubble in this inclusion contains a phase (4 × 4 μm in size) with correlation of components like that in Mg-amphibole with a Zn admixture. Its composition is as follows (wt %): 41.03 SiO_2, 0.26 TiO_2, 12.01 Al_2O_3, FeO 19.99, 6.39 MgO, 2.54 ZnO, 10.64 CaO, 0.27 K_2O, and 2.06 Na_2O (total 95.18). The Cs-rich (4.3 wt % Cs_2O) glass in MI 28/6-1a contains sheets (7 × 50 μm) of dark mica with the following composition (wt %): 42.79 SiO_2, 0.35 TiO_2, 20.15 Al_2O_3, 15.48 FeO, 0.78 MnO, 9.86 K_2O, 0.59 Na_2O, and 7.49 F. The sum total (–F = O_2) is 94.33.

Cesium is distributed uniformly in residual and quenched glasses (within the error limits). No significant correlation was established between Cs and major elements (Si, Al, Na, K, F) in the Cs-rich glasses (<7.3 wt % Cs_2O). The $Al_2O_3/(Na_2O + K_2O + Cs_2O + Rb_2O)$ molar ratio mostly is close to 1 (Table 2) and thus corresponds to the feldspathic proportions of Al and alkali metals in the melts anomalously enriched in Cs. In MI from sample ARB-28, glass with a maximum Cs_2O content (17.5 wt %) is enriched in Na and characterized by specific features of pollucite–analcime (Table 2, analysis 28/6-1).

Spherical segregations (1–5 μm) enriched in Cs and Cl relative to the adjacent glass were detected in MIs from sample ARB-24 (Table 2, analyses 24/1 and 24/1a). A Cu admixture (0.6–1.2 wt % CuO) was revealed in glasses (including the Cs-rich variety) of some MIs from sample ARB-23. The Cu content in the MI-hosted glass varies insignificantly. Some MIs contain small phases (<1 μm) with high proportions of Cu and Cl as

in $CuCl_2$. A Cl admixture (0.2–0.5 wt %) is characteristic of glasses from most MIs in all samples.

Concentrations of H_2O and some trace elements were determined with secondary-ion mass spectroscopy (SIMS) in glasses of 16 MIs, including two MIs filled with Cs-rich glass (Tables 2, 3, analyses 23/1-1 and 24/1). Glasses of all MIs are enriched in Cs, B, Be, Li, Nb, and Ta and depleted in Ba and Sr. Trace element concentrations show a wide dispersion (ppm): 122–1942 B, 16–179 Be, 73–1233 Li, 630–2705 Rb, 70–180 Nb, 11–46 Ta, 15–61 Zr, 2–7 Hf, 0.1–18 Ba, 0.3–8.0 Sr, 0.1–54 Y, 3–45 Th, 7–162 U, 1–34 La, 5–96 Ce, 1–38 Nd, and 0.01–12 Sm. Glasses of ordinary MIs contain 113–565 ppm Cs.

None of the inclusions with an anomalous Cs concentration homogenize during stepwise heating. The behavior of inclusion 23/3-1 from quartz in sample ARB-23 was studied in detail. This large (103 × 133 μm) inclusion (Fig. 1) is located in the inner zone of the quartz phenocryst together with a group of ordinary inclusions. Before the heating, this inclusion was filled with translucent glass with six gas bubbles of different diameters. A segregation of dark mica was observed in the marginal zone of inclusion. Near this inclusion, we observed tens of MIs of various sizes and filled with brown or colorless glass, one shrink bubble, and variable proportions of crystalline phases (dark mica, feldspars, and probably other minerals). After the heating to 770–800°C, only four gas bubbles were left in the glass. Glasses from other MIs became transparent, crystalline parts were partly dissolved, and a few small inclusions (2–15 μm) became completely homogeneous. At 950°C and different positions of quartz plate, a gas bubble in ordinary MIs moved freely in the vacuole and shrank. In the inclusion with an anomalously high Cs content, the bubbles remained immobile and did not shrink appreciably (Fig. 1). We also did not record complete mixing of melts in different parts of these inclusions (Tables 2, 3, analyses 23/1-1 and 23/1-1a). Near the aggregate of partially dissolved mica, the glass is depleted in SiO_2 and enriched in Al, Fe, F, and trace elements (B, Li, Nb, U, Cu, Cl. Y, and REE). The inclusions of Cs-rich glass are depleted in H_2O (~0.6 wt %) relative to the ordinary inclusions (1.5–7.0 wt % H_2O). The low water content in the Cs-rich glasses is indirectly suggested by the sum total (close to 100%) in most analyses (Table 2). The thermometric data and MI composition indicate that the viscosity of the aluminosilicate melt increases in the case of low H_2O concentrations and an anomalous Cs concentration.

Knowing the bulk Cs content in rocks and melt inclusions, one can estimate various versions of Cs fractionation during crystallization of the ongonite melt. Let us use an equation of crystal fractionation (distillation) for the case when the fluid phase is released in the course of melt crystallization and simultaneously removed from the sphere of equilibrium establishment [9]:

Table 3. Trace element and boron contents, ppm in Cs-rich glasses from melt inclusions

Element	23/1-1	23/1-1a	24/1
Cs	75292	67596	28779
B	965	1420	785
Be	90	97	24
Li	600	803	886
Rb	5010	4575	17434
Nb	116	143	84
Ta	11	26	34
Zr	28	28	36
Hf	3	4.8	5.3
Ba	18	1.9	3.1
Sr	7.7	1.4	3.3
Y	2.2	16	1.5
Th	15	32	10.4
U	106	162	13
La	7.4	23	2.4
Ce	22	54	13.8
Nd	4.5	20	2.7
Sm	1.1	6.3	0.9
Eu	0.01	0.01	0.05
Gd	1.0	6.2	1.7
Dy	1.5	8.3	1.1
Er	0.8	6.1	0.7
Yb	1.4	8.5	1.4

Note: SIMS results obtained on a CAMECA IMS-4f ion microprobe at the Institute of Microelectronics, Yaroslavl (S.G. Simakin, analyst).

$C^{Cs}_{melt} = C^{Cs}_0 (1 - F)^{D(c + fl)/melt - 1}$, where F is the content of crystals in the system (degree of melt crystallinity), C^{Cs}_0 and C^{Cs}_{melt} are the initial Cs concentration in melt and that at a given F, respectively; $D^{Cs}_{(c + fl)/melt}$ is the coefficient of Cs partition between crystals, fluid, and melt.

$D^{Cs}_{(c + fl)/melt} = x_c D^{Cs}_{c/melt} + x_{fl} D^{Cs}_{fl/melt}$, where $D^{Cs}_{c/melt}$ is the combined coefficient of Cs partition between the crystals and the melt and $D^{Cs}_{fl/melt}$ is the coefficient of Cs partition between the fluid and the melt. The x_c and x_{fl} values are mass fractions of the crystalline phases and the fluid released from the melt, respectively ($x_c + x_{fl} = 1$). Let us determine the boundary conditions for $D^{Cs}_{c/melt}$, $D^{Cs}_{fl/melt}$, x_c, and x_{fl} acceptable for Cs microadmixture in the process of ongonite melt crystallization. At 700–750°C and 1 kbar, such a melt can dissolve up to

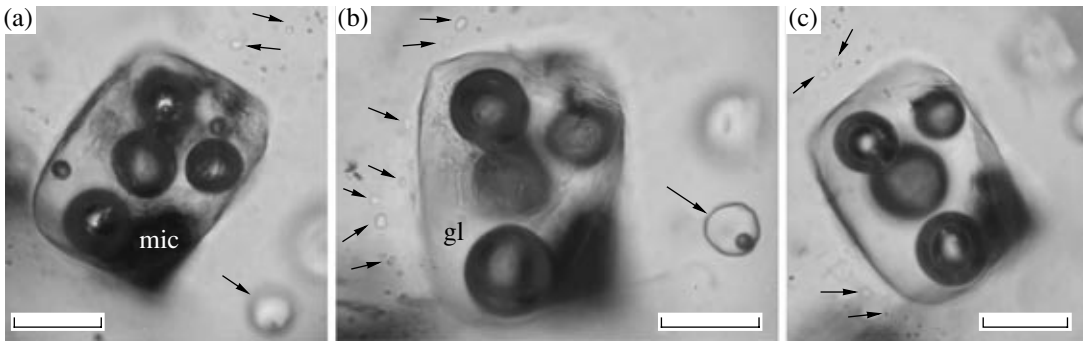

Fig. 1. Melt inclusion 23/3-1 with 7.18–7.33 wt % Cs_2O in the quenched glass after stepwise heating: (a) 7.5 h, 750°C, (b) 17 h, 750–770°C, (c) 12 h, 770–780°C and 24 h, 790–806°C. Arrows point to the ordinary melt inclusions, including homogenous glass; (mic) mica; (gl) quenched glass. Scale bar 50 μm.

10 wt % H_2O [10]. Judging from the experimental data [11], the combined partition coefficient $D^{Cs}_{c/melt}$ for acid quartz–feldspar rocks does not exceed 0.03, while the partition coefficient $D^{Cs}_{fl/melt}$ increases from 0.1 to 7.1 in response to the increase in temperature and fluid salinity. The average combined coefficient of Cs partition between minerals of phenocrysts and the groundmass of ongonites from Mongolia and one ongonite sample from Ary-Bulak Massif is 0.55 [12]. Taking the data listed above into account, the models of Cs fractionation have been calculated for an ongonite melt that contains 10 wt % H_2O at $D^{Cs}_{fl/melt} = 8$ and $D^{Cs}_{c/melt} = 0.03$ and 0.6 (without fluid release and rapid or gradual fluid release). The initial $C^{Cs}_0 = 189$ ppm in the melt is taken from the Cs contents in samples ARB-22 and ARB-23 (Table 1).

As follows from the calculation (Table 2), the melt inclusions with an anomalously high Cs content could have been captured by minerals only after the almost complete crystallization of the melt (>99.99%). This assumption contradicts the data on the degree of melt crystallization in the Ary-Bulak Massif [5], which did not exceed 40% during the growth of quartz phenocrysts before solidification of the groundmass. Crystallization of phenocrysts predated the crystallization of the groundmass. This is confirmed by Na distribution in sanidine. Sanidine phenocrysts contain less Na_2O (2.6–3.2 wt %, on average) than the rims around albite grains in the groundmass (2.8–4.6 wt %, on average; up to 6 wt % in some cases).

It is important to note that the Cs contents in the MI-hosted glass may be either higher or markedly lower than in the bulk composition of host rocks. The high concentration of Cs (up to 243–595 ppm) in the MI-hosted glass from samples ARB-24 and Arb-22 relative to the average contents (125 and 189 ppm, respectively) in the bulk rocks is attained when the melt crystallizes without release of fluid or with its insignificant loss (Fig. 2). The MI-hosted glass from sample ARB-23 contains 1.5–3.0 times less Cs (68–118 ppm) than the bulk rock (189 ppm). Such a decrease in the Cs concentration relative to its initial content in the melt may be provided only at $D^{Cs}_{(c+fl)/melt} > 1$. These conditions may be achieved in a model with $D^{Cs}_{c/melt} = 0.6$ in the case of release of a Cs-rich fluid phase and crystallization of approximately 93–97% of the melt (Fig. 2). This scenario also contradicts the available data on the degree of crystallinity during the growth of quartz phenocrysts. The presence of Cs-rich MI and the significant decrease in the Cs concentration in the MI-hosted glass (relative to the average Cs content in bulk rock) cannot be related to crystal fractionation of a homogeneous ongonite melt even under conditions of its crystallization with maximal fluid release at $D^{Cs}_{fl/melt} = 8$.

This contradiction may be resolved if we suggest appreciable Cs inhomogeneity of the melt or a great amount of excess fluid phase with $D^{Cs}_{fl/melt} > 1$. The compositional data on MIs (particularly, within one group or growth zone) allow us to infer a high degree of heterogeneity of the ongonite melt in terms of both major and rare elements. The effect of immiscibility of aluminosilicate and calcium fluoride melts revealed in Ca- and F-rich rocks of the Ary-Bulak Massif [6, 7] is also attributed to heterogenization of the ongonite melt. The presence of gas-rich inclusions (syngenetic to MIs) indicates the presence of a low-density fluid phase during crystallization of the melt. However, we cannot estimate its amount.

Thus, the data on melt inclusions show that the F- and H_2O-rich aluminosilicate ongonite melt was enriched in Cs (up to 565 ppm), as well as B, Be, Li, Rb, Nb, and Ta, at different stages of its evolution. Sporadic segregations (droplets) of the anomalous cesium melt, which was more viscous and "dry" than the ordinary ongonite magma, existed during crystallization. Some amount of Cs could have been removed from the melt along with the fluid phase.

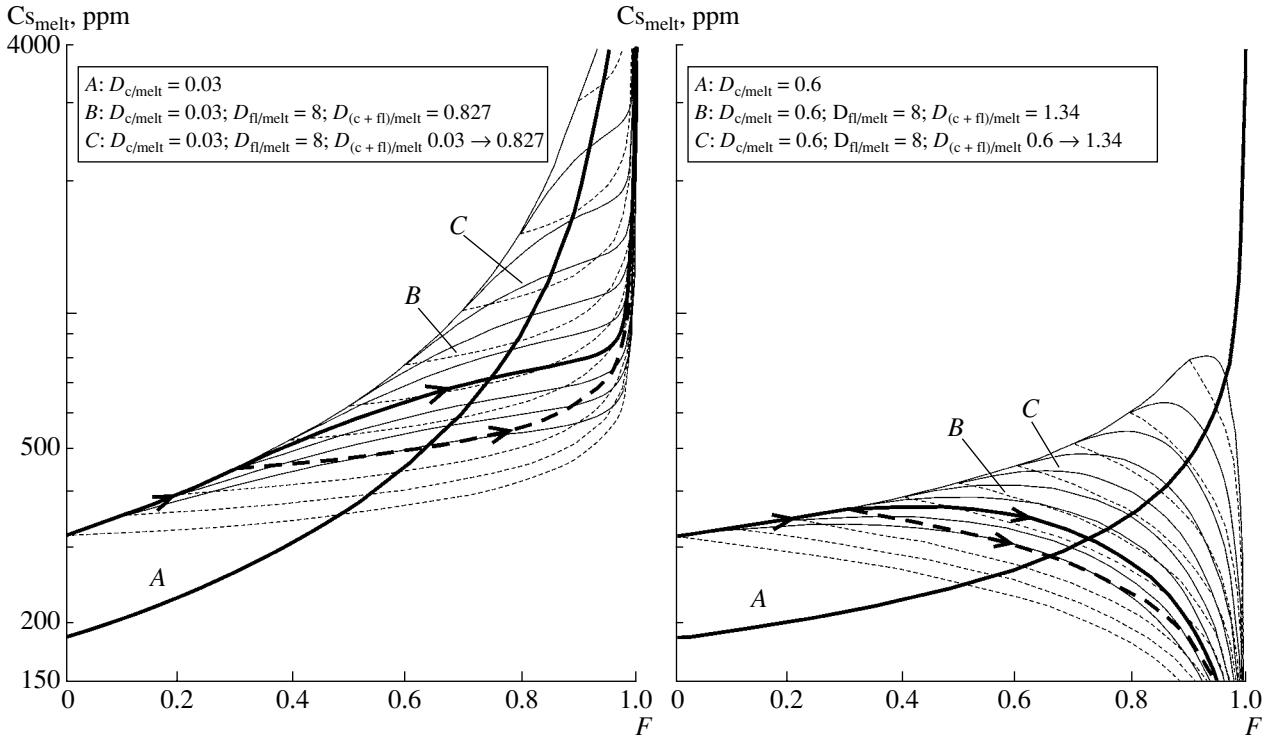

Fig. 2. Variation of Cs concentration in the melt (with 10 wt % H_2O) in the course of crystal fractionation at different $D^{Cs}_{c/melt}$, $D^{Cs}_{fl/melt}$, and $D^{Cs}_{(c+fl)/melt}$ values. (*A*) Without fluid release at constant $D^{Cs}_{c/melt} = 0.03$ and 0.6 ($C^{Cs}_0 = 189$ ppm); (*B*, dashed lines) rapid (instantaneous) removal of fluid at constant $D^{Cs}_{(c+fl)/melt} = 0.9 \cdot 0.03 + 0.1 \cdot 8 = 0.827$ and $D^{Cs}_{(c+fl)/melt} = 0.9 \cdot 0.6 + 0.1 \cdot 8 = 1.34$ ($C^{Cs}_0 = 0.9 \cdot 189 + 0.1 \cdot 8 \cdot 189 = 321$ ppm); (*C*, solid lines) with gradual loss of fluid with $D^{Cs}_{(c+fl)/melt}$ increasing from 0.03 to 0.827 and from 0.6 to 1.34 with crystallization of the melt ($C^{Cs}_0 = 321$ ppm). Heavy lines with arrows demonstrate variation of the Cs content in the melt, when the fluid phase begins to release at a degree of crystallinity $F = 0.3$ (30%).

The Cs distribution versus $D^{Cs}_{c/melt}$, $D^{Cs}_{fl/melt}$, and massif crystallization pattern observed in rocks and glasses is inconsistent with the model of fractional crystallization of homogeneous ongonite melts that may be undersaturated or saturated with fluid. This fact should stimulate in the future the development of other models, for example, crystallization of heterogeneous ongonite magma in the case of fluid flow filtration through the melt.

The mechanism of the formation of drops of aluminosilicate melt with an anomalous Cs concentration remains ambiguous. The appearance of such drops may be related to insufficient study of processes of magmatic and fluid-magmatic heterogenization of rare-metal silicic melts enriched in fluorine and fluid. The occurrence of Cs-rich melt inclusions in all studied samples indicates that this phenomenon is characteristic of the Ary-Bulak ongonite massif. The presence of similar inclusions is highly probable in minerals of not only pegmatites and ongonites, but also other Cs-rich intrusive and volcanic rocks (e.g., rare-metal granites and silicic volcanics).

ACKNOWLEDGMENTS

This work was supported by the Russian Foundation for Basic Research, project nos. 04-05-64389 and 04-05-64109.

REFERENCES

1. L. I. Lebedeva, Geokhimiya **11**, 1678 (1973).
2. S. Z. Smirnov, I. S. Peretyazhko, V. Ye. Zagorsky, et al., Dokl. Earth Sci. **392**, 999 (2003) [Dokl. Akad. Nauk **392**, 239 (2003)].
3. I. S. Peretyazhko, V. Ye. Zagorsky, S. Z. Smirnov, et al., Chem. Geol. **210**, 91 (2004).
4. I. S. Peretyazhko, S. Z. Smirnov, V. G. Thomas, et al., in *Proceedings of Int. IAGOD Conference, September 1–20, 2004* (Dal'nauka, Vladivostok, 2004), pp. 306–309 [in Russian].
5. V. I. Kovalenko and N. I. Kovalenko, *Ongonites* (Nauka, Moscow, 1976) [in Russian].

6. I. S. Peretyazhko, V. Ye. Zagorsky, E. A. Tsareva, and A. N. Sapozhnikov, [Dokl. Earth Sci. **413**, 315 (2007) [Dokl. Akad. Nauk **413**, 244 (2007)].
7. I. S. Peretyazhko, V. Ye. Zagorsky, E. A. Tsareva, et al., in *Proceedings of the 1st Meeting on Asia Current Research on Fluid Inclusions, May 26–28, 2006* (Nanjing, 2006), pp. 170–172.
8. V. S. Antipin, V. A. Kuznetsov, V. I. Kovalenko, et al., in *Proceedings of IGCP-420 on Continental Growth in the Phanerozoic: Evidence from Central Asia. IV Workshop* (Changchun, 2002), pp. 10–13.
9. I. D. Ryabchikov, *Thermodynamic Analysis of Trace Element Behavior during Crystallization of Silicate Melt*s (Nauka, Moscow, 1965) [in Russian].
10. N. I. Kovalenko, *Experimental Study of the Rare-Metal Lithium–Fluorine Granites* (Nauka, Moscow, 1979) [in Russian].
11. A. Audetat and T. Pettke, Geochim. Cosmochim. Acta **67** (1), 97 (2003).
12. V. S. Antipin, V. I. Kovalenko, and I. D. Ryabchikov, *Partition Coefficients of Rare Elements in Igneous Rocks* (Nauka, Moscow, 1984) [in Russian].